SLAC–PUB–5416
January 1991
(A)

Design of a high power cross field amplifier at X band with an internally coupled waveguide*

Kenneth Eppley and Kwok Ko

Stanford Linear Accelerator Center,
Stanford University, Stanford, CA 94309

ABSTRACT

Cross field amplifiers (CFA) have been used in many applications where high power, high frequency microwaves are needed. Although these tubes have been manufactured for decades, theoretical analysis of their properties is not as highly developed as for other microwave devices such as klystrons.

We have developed a simulation model for CFAs using the PIC code CONDOR. Our simulations indicate that there are limits to the maximum RF field strength that a CFA can sustain. When the fields become too high, efficiency becomes very poor, and the currents drawn may become so large that secondary emission cannot be maintained. It is therefore desirable to reduce the circuit impedance of a very high power tube. One method for doing this, proposed by Feinstein[1], involves periodically coupling a standard CFA circuit to an internal waveguide. Most of the power flows in the waveguide, so the overall impedance is much reduced. By adjusting the guide dimensions one can vary the impedance. Thus one can retain high impedance at the low power end but low impedance at the high power end. In principle one can maintain constant RF voltage throughout the tube.

CONDOR simulations have identified a good operating point at X band, with power generation of over 5 MW per cm and total efficiency of over 60 percent. ARGUS simulations have modelled the cold test properties of the coupled structure. The nominal design specifications are 300 MW output, 17 db gain, frequency 11.4 GHz, DC voltage 142 kV, magnetic field 5 kG, anode cathode gap 3.6 mm, total interaction length about 60 cm. We will discuss the results of code simulations and report on the status of the experimental effort.

1. INTRODUCTION

The crossed-field amplifier (CFA) is an outgrowth of the magnetron. Like magnetrons, it is capable of producing very high peak powers with reasonable efficiencies. Unlike magnetrons, the CFA is a true amplifier; however, it is difficult to obtain both high gain and low noise operation. In the CFA, electrons drift in the crossed electric field between anode and cathode and an external transverse magnetic field. A periodic structure on the anodes supports a travelling wave whose phase velocity is designed to be equal to the $E \times B$ drift velocity. RF power is injected into an input cavity, setting up a travelling wave in the anode-cathode region. With proper choice of DC electric and magnetic fields, the wave bunches the beam and produces electron spokes which interact with the field to transfer energy to it. (See Figure 1.)

Either forward or backward wave modes can be used. The backward wave CFA has the advantage that the beam sees the output cavity with its high fields first, and forms spokes quickly, while in the forward wave device a much longer distance is required before a stable spoke is

* Work supported by the US Department of Energy, contract DE – AC03 – 76SF00515.

Contributed to SPIE's Symposium on High Power Lasers,
Los Angeles, CA, January 20-25, 1991

produced. Also, the modulation of the reentrant beam has a much smaller effect in the backward wave CFA.

2. SIMULATION MODEL

Because CFA's are inherently two dimensional, non-linear devices, numerical simulation is important for accurate design. We have developed a simulation code based on the PIC code CONDOR[2] which can calculate the gain and efficiency of a CFA tube, for forward or backward wave modes, including reentrancy of the beam and secondary emission from the cathode. The main advance of our model over previous CFA simulations is the realistic tracking of absorbtion and secondary emission. The code uses experimental curves to calculate production of secondaries as a function of absorbed energy, with a theoretical term (basically $1/\cos(\theta)$) giving the angular dependence.

We simulate an interaction region, an integral number of travelling wavelengths long, with periodic boundary conditions. Time in the simulation corresponds to progression in space around the circumference of the CFA. When the beam passes out one end of the simulation box and reenters the other side, this corresponds to shifting the box one simulation length forward. (See Figure 2.)

An electric field with the appropriate phase velocity is imposed on the upper boundary (port) of the problem. We assume adiabatic change so that the port voltage V and phase ϕ depend only on the time t. We solve Maxwell's equations to obtain a self-consistent charge and field distribution.

Our calculation of the interaction between the beam and the wave is similar to that described by Yu, Kooyers, and Buneman[3]. Evaluation of the integral of $E \cdot J$ gives the power interchanged between the wave and the beam. From this power, and the impedance Z of the structure (where the power is $.5V^2/Z$), we calculate the time derivative of the travelling wave:

$$dV/dt = (Z/V) \cdot P \tag{1}$$

$$d\phi/dt = (Z/V^2) \cdot R \tag{2}$$

where P is $\int (E \cdot J d^3x)$ using the E field corresponding to phase ϕ, and R is the integral using phase $\phi + \pi/2$.

For a backward wave mode, the beam enters at the high power output and proceeds to the input. In simulating the backward mode, power is extracted from the wave as the beam progresses from output to input. We assume some output power level, and calculate what input level would be needed to produce this. Steady state is assumed, so that we can ignore the fact that the group velocity is different from the particle drift velocity.

The beam is reinjected after passing through the sever to determine the effect of starting with an initially modulated beam. Generally, successive passes will not exactly reproduce, especially in the low voltage section, due to space charge oscillations which are at a different frequency than the operating frequency. Real devices tend to average out phase variations over the third dimension, so our calculations tend to overestimate the phase jitter in the low voltage section.

It is sometimes useful to run the code with the RF voltage fixed, turning off the interaction. This is helpful to calculate curves of power generation versus RF and DC voltage, etc. It is also the only way at present that we can model actual vane structures, since we do not have an analytic form for the fields between the vanes.

The initial simulation model included only the synchronous harmonic. The wavelengths of the other harmonics are, in general, not simply related to the synchronous wavelength, and would not be correctly modelled by the periodic boundary conditions in the simulation. However, for certain specific phase shifts, where the ratio between wavelengths is a simple fraction, e.g., 1/2 or 2/3, it is possible to model more than one harmonic with a longer simulation region and still use periodic boundaries. For example, consider a fundamental wave with -120 degree phase shift per resonator. The first harmonic has β = -120 + 360 = +240 degrees. One can model both harmonics using a simulation region of one fundamental wavelength (three resonator lengths). For 120 degrees, because the simulation covers an integral number of resonators, one can model all harmonics, either as separate terms or by modelling the voltage across the vanes with RF ports.

Another possibility is to use a fundamental with phase shift of -144 degrees, with a harmonic of +216 degrees. The fundamental wavelength is 3/2 the harmonic wavelength, and one can model these two modes in three harmonic wavelengths. Likewise, with five wavelengths we can model the two modes -135 and +225 degrees.

The code also now permits variable phase velocities. To keep the simulation region equal to one wavelength, the zone size has to be varied continuously, and all the quantities related to the zone size have to be recalculated on every timestep. The particle coordinates do not change, so there may be either too many or too few particles at the left and right boundaries when the mesh is altered. This does not seem to create a problem as long as the change per time step is small.

When we vary β as a function of time, we use empirical measurements to determine the scaling of the group velocity v_g as a function of β. From this we calculate the scaling in the impedance and attenuation. The RF voltage must change as the impedance is varied to conserve energy:

$$\delta V_{rf} = V_{rf} \cdot \delta Z/(2Z) \tag{3}$$

3. MAXIMUM RF FIELD LIMITATIONS

CFA's have been observed to have an "upper mode current cutoff," i.e., a maximum level of current they can support. We have found two mechanisms which can limit cathode current emission. For high enough RF fields, the cathode bombarding energy can become so large that the secondary emission ratio goes below unity. The material having the highest value at which this occurs is platinum, at 6 keV. (See Skowron[4]). If most of the deposited electrons are above this threshold, secondary emission will not maintain the hub current.

A cutoff of secondary emisssion can also occur from a different mechanism. When the RF field exceeds a threshold, which depends on the DC voltage, gap width, and DC magnetic field, the spoke draws so much current that the hub is depleted and secondary emission ceases (Figure 3).

When the synchronous mode is the fundamental, we have found that the second mechanism (spoke depletion) is more important than the first one (exceeding secondary threshold). Even though the synchronous voltage may be tens of kV, space charge oscillations in the hub can produce many low energy electrons which hit the cathode. The bombardment energy distribution is peaked at low energies (a few tens of eV) and falls off monotonically with energy, with the

median absorbed energy being roughly half the mean value. Thus an oxide cathode (e.g., BeO) may allow higher peak power than platinum, since such cathodes have higher secondary yield and lower peak energy. Simulations verified this for a synchronous fundamental.

In the initial SLAC CFA the fundamental mode was -135 degrees, with longer wavelength than the synchronous mode of 225 degrees. The fundamental amplitude at the anode was about the same as the synchronous wave, but at the cathode it was considerably stronger, since the decay constant is proportional to wavelength. We found that at high power levels, the high transverse fields at the cathode from the fundamental could increase the bombardment energies above the maximum threshold for secondary emission. Then cutoff occurred at a much lower RF power level than for the synchronous wave alone.

4. ANODE DISSIPATION

One limitation on the peak power level is due to absorbtion of power by the anode. If the anode temperature goes too close to the melting point during the duration of the pulse, the surface will be damaged and the lifetime of the tube will be short. The temperature rise for a copper anode is given by

$$\Delta T = .311 \cdot P \cdot \tau^{1/2} \tag{4}$$

where T is in degrees C, P is power absorbed in watts/cm^2, and τ is the pulse width in seconds. For copper the temperature rise should be limited to about 600 degrees C to maintain acceptable lifetimes. For a 100 ns pulse the power must be less than 6 MW/cm^2 for ΔT to be below 600 degrees. If the anode vanes are tipped with tungsten, the temperature rise will be higher, but the melting point is also higher, and the allowed dissipation will be about double that for uncoated copper.

McDowell[5] found that proper shaping of the anode vanes could reduce dissipation. We studied this with simulations which included the vane structure (with fixed RF voltage). We did not find any advantage to beveling the edges of the vanes, as McDowell had proposed. Generally, we observed that when the RF voltage across the slot exceeds the DC voltage, electrons are turned around between the vanes and strike the upstream edge with high energy, increasing anode heating and reducing efficiency. At lower RF levels, electronic efficiencies in excess of 70% are attainable.

5. APPLICATION TO INITIAL SLAC X BAND CFA

The X-band CFA tested at SLAC, designed by Joseph Feinstein and Terry Lee, has been described elsewhere[6]. The tube was intended to produce 100 MW, but actually made only 10 MW. Our simulations gave some explanations for the low power level. One major problem was a failure to reach the desired operating voltage of 140 kV. Arcing limited it to less than 100 kV. Also, the desired mode of 135 degrees was misidentified in the cold-test model, and this mode was at about 12 GHz instead of 11.4 GHz. The driver could only reach about 11.7 GHz, at about 120 degrees. Calculations of the circuit impedance by Nelson using the QUAP code showed that it was actually a factor of two higher than the original estimate, which reduced the peak rf power the tube can support. As discussed above, the non-synchronous fundamental mode increased the cathode bombardment energy and further reduced the peak RF power.

Putting all these effects into the simulation model, we found that when the power level became too high (20-30 MW at the optimal operating point, 10-15 MW at the best experimentally obtainable point), the transverse fields at the cathode raised the bombardment energy and cut off secondary emission.

The tube was rebuilt with larger end hat and anode-cathode spacings, and the resonators were machined to bring the 135 degree mode down to 11.4 GHz. Unfortunately, by mistake it was brought down too far, to 11.2. The code predicted that about 20 MW should be produced. Although the tube was able to hold off higher voltages, its RF output was only a few MW. The V-I curve was not consistent with a 225 degree phase shift, and Feinstein suggested that it was operating as a forward wave device at 135 degrees. However, reversing the magnetic field produced almost no current at all. We have not yet explained this.

6. CFA WITH INTERNALLY COUPLED WAVEGUIDE

We attempted to find a better design using a synchronous fundamental which would give a good rate of power generation with high efficiency and low anode dissipation. We found a good operating point (see Figure 4 and table below). However, a conventional resonator circuit with these dimensions has such a high impedance that this RF voltage is only about 15 MW output power. Feinstein suggested that a structure coupled through slots to an internal waveguide, which has been used successfully in some tubes, would lower the impedance by a large factor. (See Figures 5 and 6.) By varying the depth of the waveguide, one can taper the impedance. It is desirable to have the impedance as high as possible near the input, and low near the output. This allows a higher gain and more efficient use of the tube, if one could choose the taper to keep the RF voltage near the optimum level. The impedance variation should reduce problems with current depletion, anode heating, and breakdown at the output, and improve power production and phase stability at the input.

A constant RF voltage implies a contant power generation rate and thus a taper on Z inversely proportional to distance, i.e., with the guide dimension linear in distance. A simulation assuming such a linear variation was able to keep the RF field nearly constant over a large range of power levels, with total efficiencies of close to 70%. The curves of power production versus RF voltage become fairly flat at higher levels, so small variations should not be a problem.

An important issue in a waveguide-coupled circuit is the contamination of the operating mode by nearby undesireable modes. Mode purity can be maintained if the circuit is matched. At the match point the voltages across both coupled and uncoupled resonators will be equal. A match point occurs when the tangential electric field at the junction between the resonator and the waveguide coupling slot is zero. Then we can replace the junction by a conductor and separate the geometry into the usual anode circuit and the slotted guide. We then design each circuit individually for the appropriate phase shift at the correct frequency, 150 degrees for the anode and 60 degrees for the slotted guide, both at 11.4 GHz. We obtain the final design by coupling the two circuits and make small adjustments to correct for any frequency shift.

The desired impedance at the 300 MW level is about 17 ohms. Nelson added quasi-periodic boundary conditions to ARGUS, allowing it to calculate the impedance of the structure. The calculations showed that the 17 ohms can be obtained with a guide depth of about .4 inches. A 3 MW input power level at the same RF voltage would correspond to 1700 ohms, which is not attainable with a coupled structure. It could be achieved with an uncoupled structure, but the transition between coupled and uncoupled circuit might produce reflections. The coupled structure impedance can reach a maximum of about 200 ohms. There is also a phase shift of about eight degrees with this higher impedance, which fortunately is in the right direction to lower V/V_H at the lower RF field strengths. Simulations with such an impedance and phase variation indicated a drive requirement of about 6 to 8 MW.

We note that this circuit uses a backward wave mode, but the synchronous mode is the fundamental, so it should not possess the problems we believe limited the first tube. ARGUS cold-test simulations have examined potential problems such as the possibility of trapped slot modes and possible longer wavelength harmonics due to the fact that the coupling slots are not connected to every resonator. At the operating mode, the voltages across the alternate resonators are quite uniform, so the longer wavelength harmonic appears too weak to interfere with cathode emission. However, ARGUS identified a mode of another frequency which can interact with the beam with a high impedance (Figure 5). CONDOR simulations including this mode (at low amplitude) and the operating mode together showed that the competing mode had enough gain to reach high power levels and interfere with the tube operation. Feinstein suggests that lossy material can be inserted to damp out this mode while having little effect on the desired mode.

7. TABLE OF TUBE SPECIFICATIONS

Cathode dimensions: radius $r_c = 10.16$ cm; height $h_c = 1.65$ cm
Anode dimensions: radius $r_a = 10.52$ cm; height $h_a = 1.65$ cm
Anode-Cathode gap: $g = 3.63$ mm
Pitch: $p = 2.67$ mm
Vane dimensions: height $h_v = 1.65$ cm, depth $l_v = 4.98$ mm
Vane gap width: $d_1 = 1.016$ mm; $d_2 = 2.032$ cm; triangular
Waveguide dimensions: height $h_w = 1.905$ cm; depth $l_w = .762$ to 7.62 cm
Slot dimensions: height $h_s = 1.905$ cm; depth $l_s = 4.57$ mm; width $d_s = .508$ mm
Frequency: 11.424 GHz
Peak Power Output: 300 MW
Power Generation Rate: 6 MW per cm of circumference
RF Pulse Width: 100 ns
Pulse repetition rate: 360 pps
Anode Voltage: 142 kV
Anode Current: 2600 Amp
Peak RF Voltage Across Vanes: 100 kV
Efficiency $\eta_e \cdot \eta_c = .72 \times .9 = 0.65$
Gain: 17 db
RF Drive Power: 6 MW
Emitter: Beryllium Oxide cold cathode
Cathode current density: 41 Amp/cm^2
Number of anode resonators: 225
Average anode dissipation: 40 W/cm^2 at 100 ns
Peak anode dissipation: 1.1 MW/cm^2
Mean anode bombardment energy: 27 kV
Phase shift per resonator: 150 degrees
Phase velocity: $7.31 \cdot 10^7$ m/s
Hartree voltage: 118 kV
DC magnetic field: 5 kGauss

8. REFERENCES

1. J. Feinstein and R. Collier, "A Class of Waveguide-Coupled Slow-Wave Structures," *IRE Transactions on Electron Devices,* pp. 9-15, January, 1959.

2. B. Aiminetti, S. Brandon, K. Dyer, J. Moura, and D. Nielsen, Jr., *CONDOR User's Manual,* Livermore Computing Systems Document, Lawrence Livermore National Laboratory, Livermore, California, April, 1988.
3. S. Yu, G. Kooyers, and O. Buneman, "Time-Dependent Computer Analysis of Electron-Wave Interaction in Crossed Fields," *Journal of Applied Physics, 36,* 8, pp. 2550-2559, August, 1963.
4. J. Skowron, "The Continuous Cathode (Emitting Sole) Crossed Field Amplifier," *Proceedings of the IEEE, 61,* 3, pp. 330-356, March, 1973.
5. H. McDowell, *CFA Design Improvement Program: Part II, Final Report, Volumes I and II,* Varian Associates, Inc., Beverly, Mass., June, 1982.
6. K. Eppley, "Numerical Simulation of Cross Field Amplifiers," *Proceedigns of the Conference on Computer Codes and the Linear Accelerator Community,* Los Alamos, N.M., January 22-25, 1990.

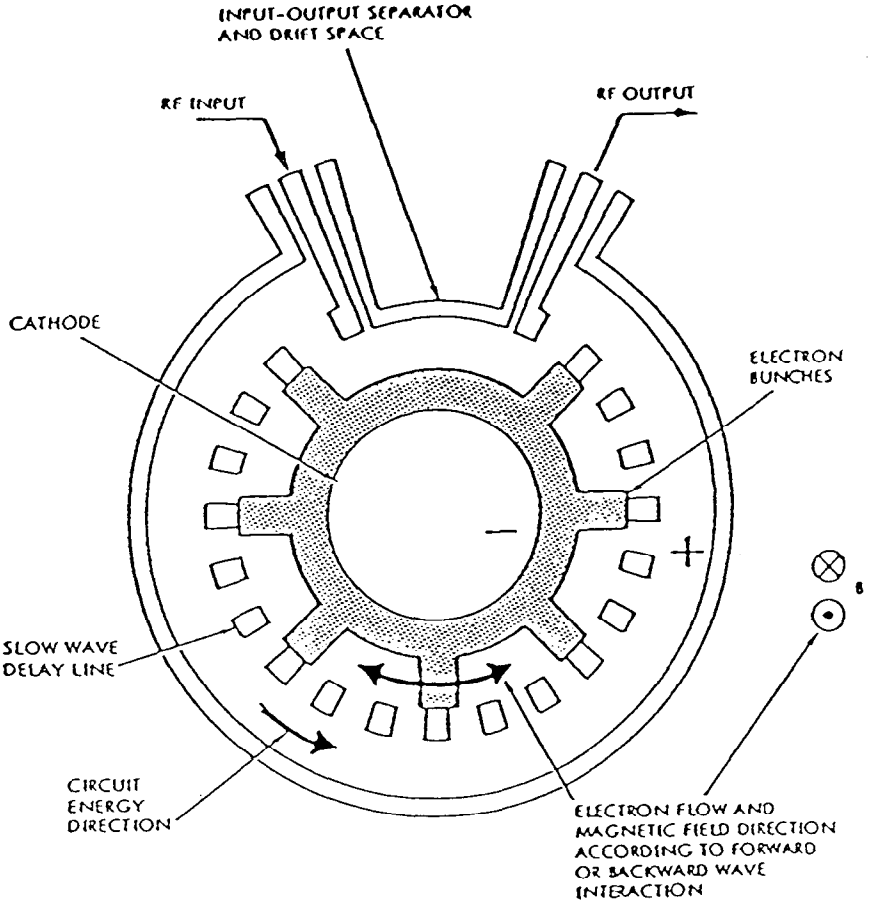

Figure 1. Schematic of a CFA showing vanes, input, output, and sever (drift space with no RF which isolates input and output).

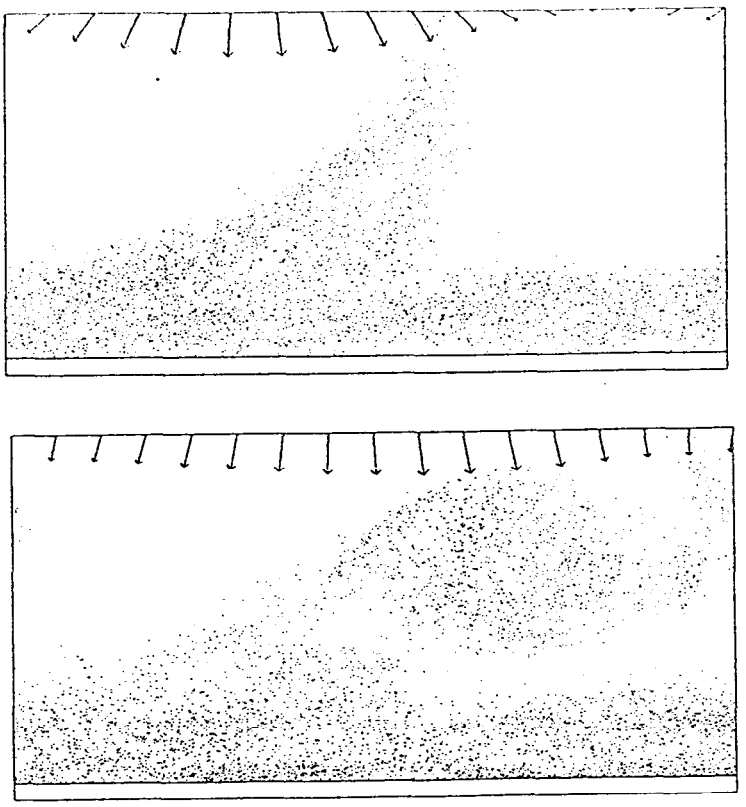

Figure 2. Simulation of one (slow wave) wavelength of electron position-space distribution showing electron hub and spoke. The horizontal axis is Z and the vertical axis is R. (Center line is axis of symmetry.) DC plus RF field vectors are plotted at the anode. The boundary conditions are conducting on the bottom, metal with imposed travelling voltage on top, and periodic on the sides. The top picture shows a strong RF field which holds the spoke tightly, while the second shows a weaker field where the spoke undergoes tumbling.

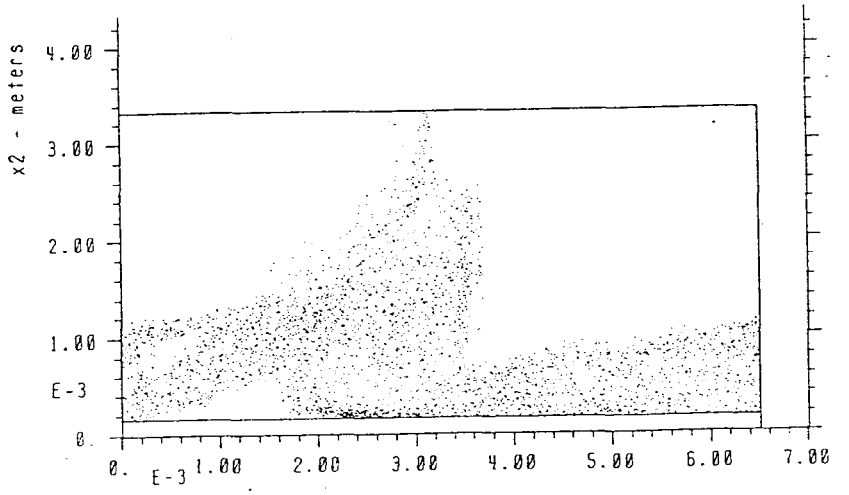

Figure 3. Onset of current depletion. Peak RF field was 77 MV/m, DC voltage 140 kV, magnetic field 6 kGauss, anode-cathode gap .32 mm.

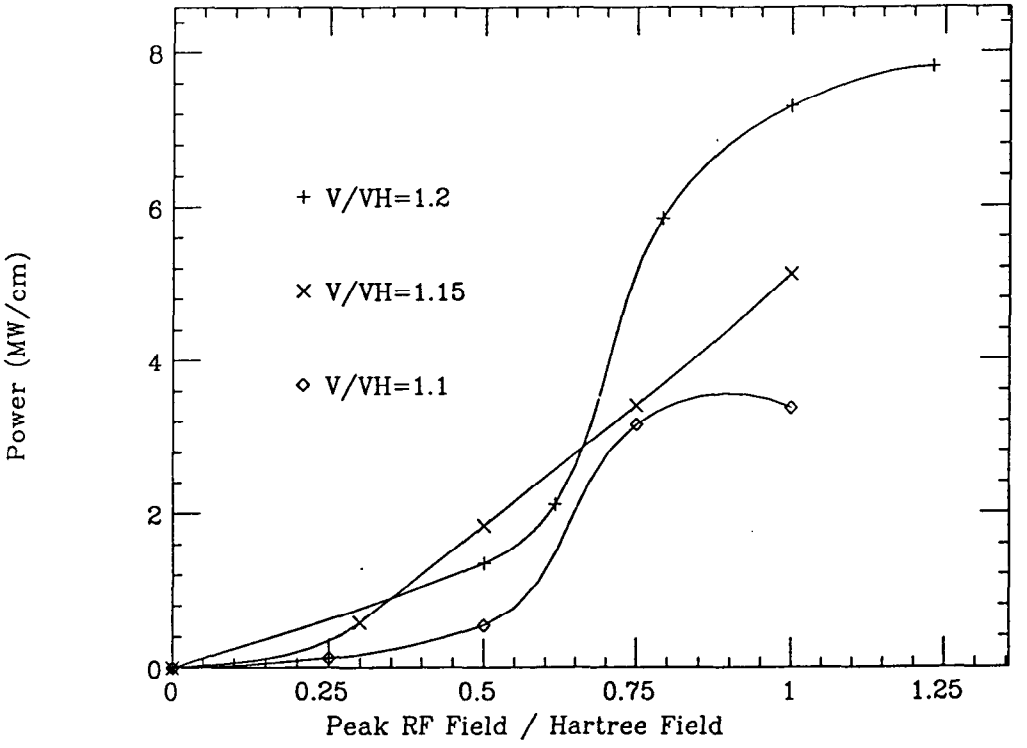

Figure 4a. Power generation rate (MW/cm) vs. normalized RF field strength, $(V_{RF}/d_1) \div (V_H/g)$, where d_1 is vane slot width and g is a-k gap. Shown for three values of DC voltage. Values were calculated for the design given in the table.

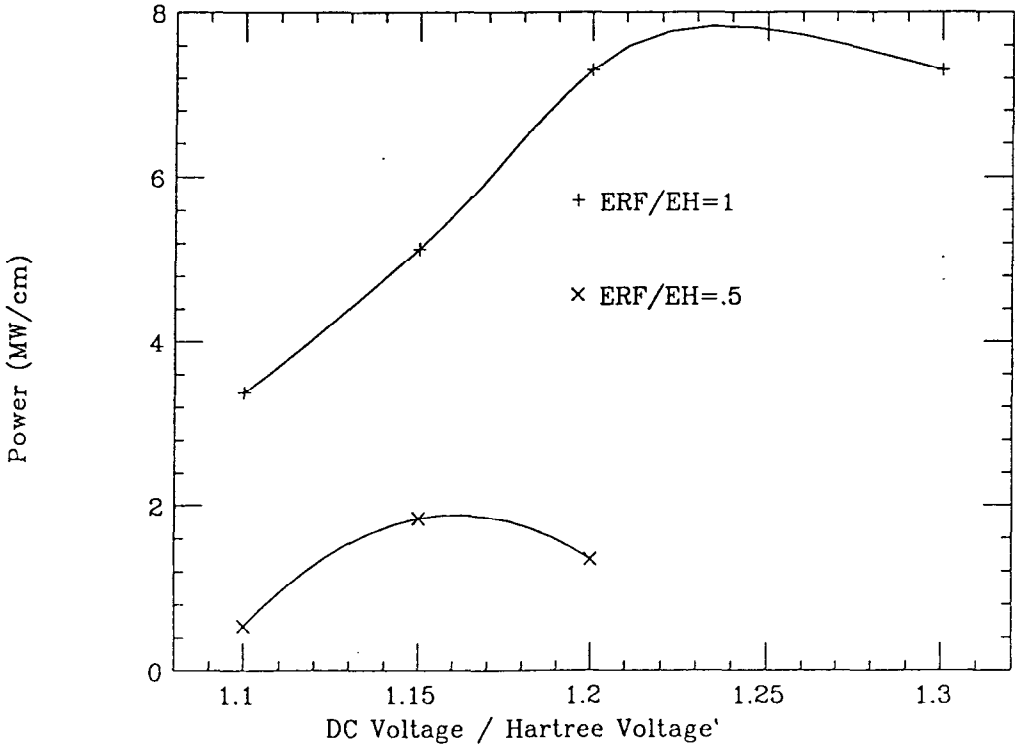

Figure 4b. Power generation (MW/cm) vs. V/V_H.

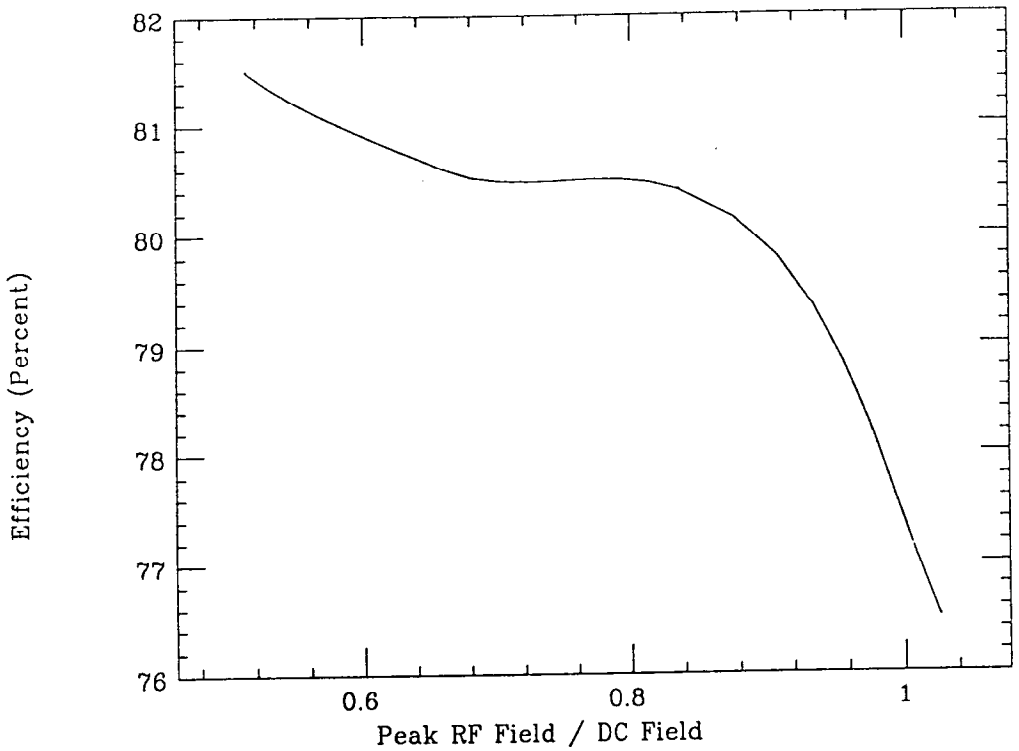

Figure 4c. Efficiency vs. normalized RF field strength.

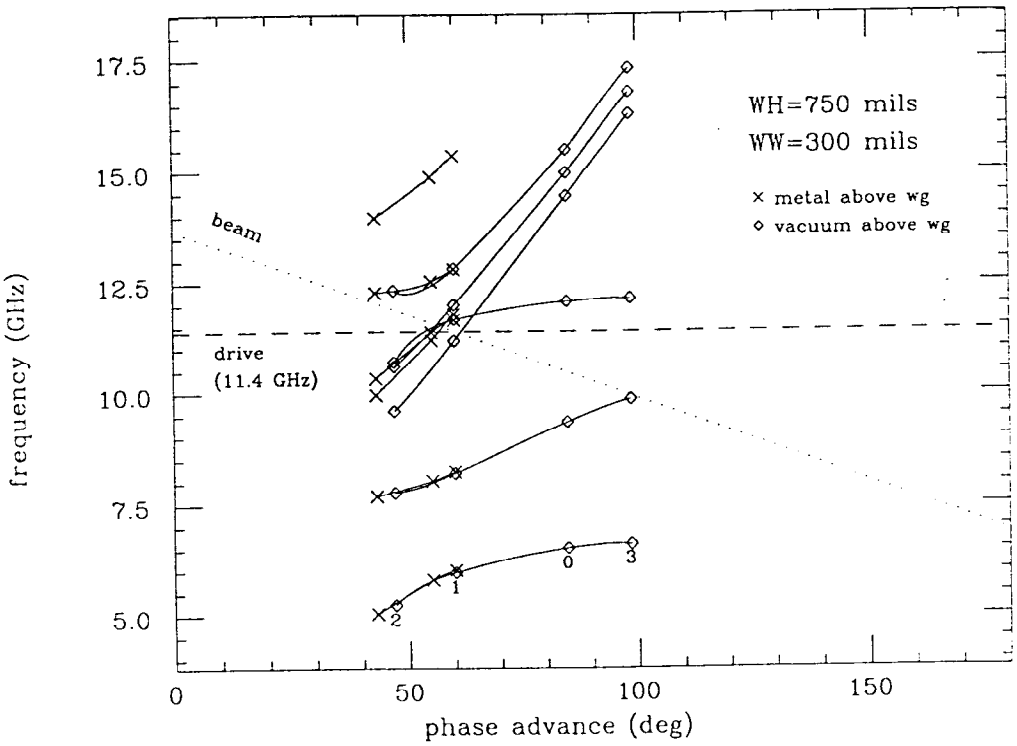

Figure 5. Dispersion curve for coupled structure.

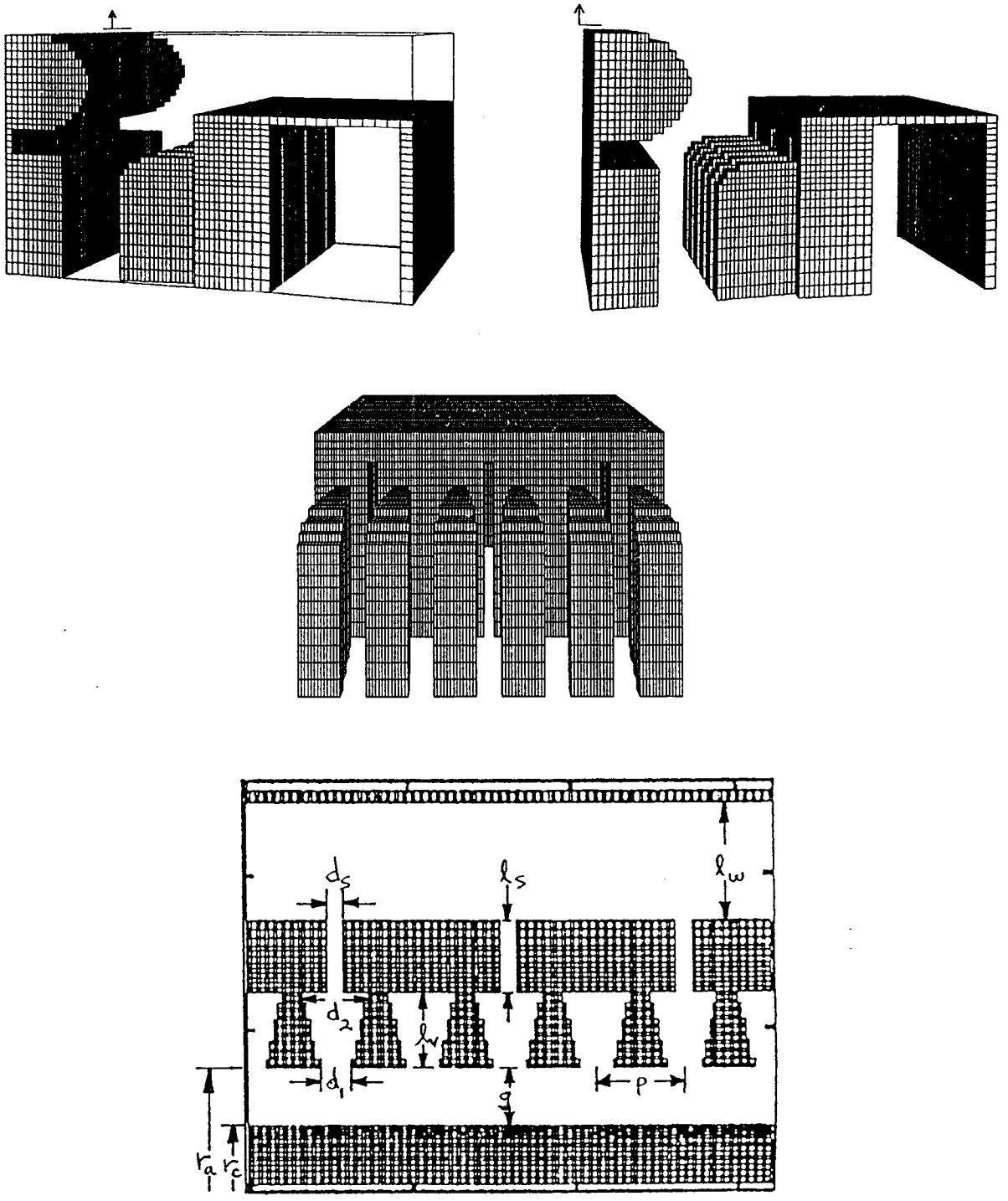

Figure 6. ARGUS model of waveguide coupled structure. The circuit is shown from several perspectives. See the table for values of the dimensions.